



# Abundance of *Vibrio aestuarianus*, water temperature, and stocking density are associated with summer mortality of Pacific oysters in suspended culture

M. W. Cowan<sup>1,2,3</sup> · C. M. Pearce<sup>2</sup> · T. J. Green<sup>3</sup> · T. Finston<sup>1</sup> · G. R. Meyer<sup>2</sup> ·  
B. McAmmond<sup>4</sup> · J. D. Van Hamme<sup>4</sup> · E. M. Bottos<sup>4</sup> · R. Marshall<sup>5</sup> · W. Evans<sup>6</sup> ·  
T. F. Sutherland<sup>7</sup> · P. Y. de la Bastide<sup>1</sup>

Received: 15 November 2023 / Accepted: 25 January 2024  
© Crown 2024

## Abstract

High mortality rates of cultured Pacific oysters (*Crassostrea gigas*) during the summer months have regularly occurred on oyster farms in British Columbia, Canada over the last 10 years, but little is known about the microbial and environmental conditions that contribute to such mortality events. The objective of the study was to determine correlative factors associated with the onset of a summer mortality event in oysters (mean  $\pm$  SD shell height:  $14.2 \pm 0.5$  mm) grown in suspended culture at four stocking densities (150, 300, 450, 600 oysters tray<sup>-1</sup>) from May 11 to September 17, 2018. Variables examined included both biotic (oyster growth, mortality, reproductive development, and microbiome (approximately every week); *Vibrio* and harmful algal species abundance) and abiotic (temperature, salinity, turbidity, dissolved oxygen,  $p\text{CO}_2$ , pH, and aragonite saturation) ones. Both the absolute abundance of *V. aestuarianus* and the relative abundance of *Vibrio* spp. increased with observed oyster mortality and declining health. Mortality was highest on August 12 and associated with a prior period of elevated temperatures (i.e., increasing temperatures from early July to early August) and increased oyster growth/reproductive development. At that time, systemic mixed microbial infections and necrotic gill tissue in histological cross sections were observed in 19% of oysters that appeared healthy macroscopically. Cumulative percent mortalities per tray ranged from 34 to 75%, the highest-density trays having significantly less mortality and smaller shell width, shell length, and gonad length than lower-density trays. This study demonstrates the significant impact of summer mortality on Pacific oysters and highlights the biotic (host growth, reproductive development, and microbiome composition as well as *Vibrio* spp. abundance) and abiotic (water temperature) factors associated with the observed mortality in this region.

**Keywords** Bacterial pathogens · Marine heatwaves · Microbiome · Oyster mortality events · Shellfish aquaculture

---

Handling Editor: Gavin Burnell

Extended author information available on the last page of the article

## Introduction

Pacific oysters (*Crassostrea gigas*) are one of the most extensively cultured bivalve species in the world (FAO 2018). In British Columbia (BC), Canada, Pacific oysters have been an important farmed species for over a century and have a significant socio-economic role in coastal communities (Quayle 1988; DFO 2013). Oyster aquaculture in Baynes Sound, BC generally relies on hatchery-produced seed grown in suspended culture for their first year, followed by shell hardening on an intertidal beach before being sold on the half-shell market. Baynes Sound is a small passage between Vancouver Island and Denman Island that is extensively farmed, with 137 shellfish tenures that include 90% of the intertidal area (Bendell 2019), although not all farms are always active. In recent years, the BC oyster aquaculture industry has been faced with recurring summer mortalities of unknown aetiology. Typically, these mortality events can cause losses of 20–100% of the farmed product throughout the summer. High temperature, reproductive development, and opportunistic pathogens are well-studied factors that have been implicated in Pacific oyster summer mortality in other regions of the world (Katkansky and Warner 1974; Garnier et al. 2007; Wendling and Wegner 2013; Azéma et al. 2016; Green et al. 2019), but little is known about the causative factors in BC (Cowan et al. 2023).

Summer mortality events generally occur during periods of elevated temperature and reproductive effort (Cotter et al. 2010; Wendling and Wegner 2013). The process of gametogenesis and spawning in Pacific oysters is energy-intensive, their gonads developing rapidly and accounting for over 50% of their body volume when fully developed (Imai et al. 1965; Quayle 1988). During that period, oysters may have a compromised immune system with reduced thermo-tolerance and anti-microbial activity (Li et al. 2007; Huvet et al. 2010; Wendling and Wegner 2013). The intensity of reproductive effort has been positively correlated with the susceptibility of Pacific oysters to summer mortalities in both field (Imai et al. 1965; Perdue et al. 1981; Cotter et al. 2010) and laboratory (Delaporte et al. 2007; Huvet et al. 2010; Wendling and Wegner 2013) studies. Further, gonadal tissue may be more susceptible to infections by opportunistic pathogens, such as *Vibrio* spp. (De Decker et al. 2011).

Bacterial pathogens have been considered a key factor in some Pacific oyster summer mortality events. The most well-documented bacteria associated with oyster mortalities include *Vibrio aestuarianus* and *V. splendidus*, both implicated in mass mortalities in various commercial farms in France (Lacoste et al. 2001; Garnier et al. 2007; Barbosa-Solomieu et al. 2015; Azéma et al. 2016), and *Nocardia crassostrea*, involved in summer mortalities in Puget Sound (Washington, USA) and Nanoose Bay, Denman Island, and Scott Island (BC) (Elston et al. 1987; Friedman et al. 1991; Friedman and Hendrick 1991). Although the genus *Vibrio* contains several opportunistic pathogens affecting humans and many marine species (Baker-Austin et al. 2018), *V. aestuarianus* is associated with significant mortalities in Pacific oysters, older individuals being most susceptible (Azéma et al. 2016). In other regions of the world, changes in oyster microbial community structure (particularly increases in *Vibrio* spp. abundance) coincide with summer mortalities, providing evidence of their association with summer mortality events (Green et al. 2019; King et al. 2019b, c).

Diverse and stable microbiomes are important for host immunity and can protect them from colonization by pathogens (Kamada et al. 2013). Pacific oyster microbiomes typically decrease in diversity when disease symptoms are observed (Lokmer and Wegner 2015; Green et al. 2019; King et al. 2019b). The use of high-throughput

sequencing targeting the 16S rRNA gene provides an effective way to assess changes in microbial communities associated with Pacific oyster summer mortality (Wendling et al. 2014; Green et al. 2019; King et al. 2019b). For example, King et al. (2019b) demonstrated an increase in rare operational taxonomic units (OTUs), belonging to *Vibrio harveyi* and another unidentified *Vibrio* sp., in the microbiomes of diseased oysters compared with those in healthy oysters.

Alteration of the culture density of oysters may be a potential method to mitigate summer mortalities because high culture densities potentially reduce oyster growth rate and reproduction by limiting food availability and space (Chávez-Villalba et al. 2010). A reduction in food concentration has been shown to reduce the reproductive effort of oysters and resulted in reduced mortalities in controlled experiments (Delaporte et al. 2007; Enríquez-Díaz et al. 2009). Conversely, higher densities may contribute to higher mortalities due to competition for space and resources and/or to increased transmission of pathogenic agents between hosts (Baker-Austin et al. 2018).

Literature on Pacific oyster summer mortality suggests that it is a complex multifactor disease progression with several different cumulative sublethal stressors contributing to the susceptibility by opportunistic disease agents (King et al. 2019b). That could include harmful algal species such as *Alexandrium* spp. that increase the susceptibility of oysters to infections by *V. tasmaniensis* (Abi-Khalil et al. 2016). Similarly, exposure to adverse environmental conditions or variability can cause diseases and mass mortalities of oysters (King et al. 2019a).

The present study evaluates the role of both biotic (oyster growth, reproductive development, microbiome, and stocking density; *Vibrio* abundance; harmful algal species and concentrations) and abiotic (temperature, salinity, turbidity, dissolved oxygen,  $p\text{CO}_2$ , pH, and aragonite saturation) factors in summer mortality of Pacific oysters grown in suspended culture at four different densities (150, 300, 450, 600 oysters tray<sup>-1</sup>). Two key questions were addressed: (1) does oyster stocking density influence the timing and magnitude of oyster mortality and (2) does the microbiome of oyster gill tissue change over the course of the summer and during periods of elevated mortality?

## Materials and methods

### Experimental design

This investigation was conducted in Metcalf Bay, Baynes Sound, BC (49.250° N, 124.456° W) (Fig. 1) from May 11 to September 17, 2018 using the commercial practices of suspended oyster culture in the region. Oysters at the start of the experiment were  $14.2 \pm 0.5$ ,  $4.7 \pm 0.2$ , and  $11.0 \pm 0.3$  mm (mean  $\pm$  SD) in shell height, width, and length, respectively, and 8 months in age. They were placed in Dark Sea oyster trays (L  $\times$  W  $\times$  H: 69  $\times$  69  $\times$  9 cm) at four different common commercial stocking densities (150, 300, 450, 600 oysters tray<sup>-1</sup> or 71.4, 142.8, 214.3, 285.6 oysters m<sup>-2</sup>) with four replicate trays per density, for a total of four blocks in a Latin square design (Supp. Fig. 1). The blocks of trays were suspended from rafts in the water column at 5-m depth (at mid-point of the block) and 1.5 m apart horizontally.

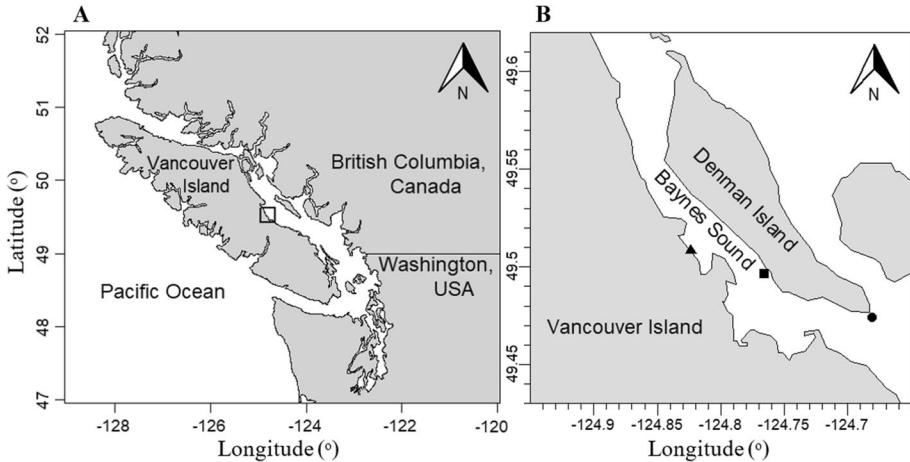


**Fig. 1** **A** Map of Pacific Northeast with the field site location shown with a square. **B** Baynes Sound showing Metcalf Bay in black square (■), Fanny Bay in black up-pointing triangle (▲), and Chrome Island in black circle (●)

## Environmental factors

A YSI EXO2 multiparameter water quality sonde (YSI, Yellow Springs, OH, USA) was deployed at 5-m depth in Fanny Bay ( $49.507^{\circ}$  N,  $124.829^{\circ}$  W), 6.7 km from the field site, for the duration of the experiment and measured temperature, salinity, turbidity, and oxygen saturation at 10-min intervals. An Onset® HOBO® pendant (Onset, Bourne, MA, USA) was attached to an experimental tray block (in Metcalf Bay only) at mid-height and recorded temperatures at 10-min intervals. Daily water temperatures at the Chrome Island lighthouse ( $49.496^{\circ}$  N,  $124.765^{\circ}$  W, 6.5 km from the field site) from 1969 to 2018 were downloaded from the Department of Fisheries and Oceans (DFO 2019).

Eleven water samples were periodically (every 6–12 d) collected throughout the summer for carbon chemistry analysis in 350-ml soda-lime glass bottles from surface water (0 m) directly above the trays, care being taken to limit the introduction of air bubbles (Evans et al. 2019). Bottles were preserved with 200  $\mu$ l of a saturated mercuric-chloride solution and capped with polyurethane-lined metal caps. Samples were analyzed using a Burke-o-Lator (Hales et al. 2004), and partial pressure of carbon dioxide ( $p\text{CO}_2$ ), temperature-adjusted hydrogen ion concentration ( $\text{pH}_T$ ), and aragonite saturation state ( $\Omega_{\text{arag}}$ ) computed using the CO2SYS program on MATLAB (Van Heuven et al. 2011; Evans et al. 2019).

## Oyster monitoring and collection

Approximately every 2 weeks between May 11 and September 17, 2018, the shell height, length, and width of 10 haphazardly-selected oysters from each tray were measured. Dimensions used were described by Galstoff (1964): height is the distance between the umbo and the ventral valve margin, length is the maximum distance between the anterior and posterior margin parallel to the hinge axis, and width is the greatest distance between the top and bottom shell halves. To assess mortality, 100 haphazardly-selected oysters from each tray were examined. Dead oysters were defined as those with no shell-closing response. Live and dead oysters were both returned to the trays after counting. Starting on

May 23, and on a total of nine sampling dates, one oyster that appeared healthy was haphazardly collected from each tray ( $N=16$  per sampling date,  $N_{\text{total}}=144$ ) for microbiome and histological analysis. Oysters were scrubbed with a bristle brush to remove biofouling, then opened using a shucking knife and scalpel that were disinfected for approximately 2 min in 70% v/v ethanol between processing each oyster. A transverse cross section (~3 mm thick) was cut through the visceral mass of each oyster and preserved in Davidson's solution for histological examination (Howard et al. 2004). A small piece of gill tissue was removed and preserved in 500  $\mu\text{l}$  of RNALater (Invitrogen, Carlsbad, CA, USA) and stored at  $-80\text{ }^{\circ}\text{C}$  for later DNA extractions.

## Histology

Transverse tissue cross sections were taken perpendicular to the dorsal–ventral margin from healthy oysters, which included gill, stomach, labial palps, and gonad tissue, and they were processed using routine histological techniques and embedded in paraffin. Five- $\mu\text{m}$ -thick tissue sections were de-paraffinized, rehydrated, and stained with Harris' modified hematoxylin and eosin (H&E) stain. Tissue sections from the 16 healthy oysters sampled on August 12 (during the mortality event) were also stained with Gram stain.

Histology slides were examined via light microscopy and the gonad development of each oyster was categorized based on the stages described by Steele and Mulcahy (1999): undifferentiated (0), early active (1), late active (2), ripe (3), partially spent (4), totally spent (5), post-spawning (6), and resorption (7). Images of each oyster cross section were captured via light microscopy and traces of gonad area (GA) and total oyster area (OA) were prepared on QGIS (QGIS 2020). The GA, OA, and maximal gonadal length (GL) of each oyster were quantified using ImageJ software (Schneider et al. 2012), and the gonadosomatic index (GSI) was calculated as the proportion of GA to OA. In addition, the histology slides were examined for the presence of pathogens and pathology.

## DNA extraction

In addition to the 16 gill clippings collected per sampling date, two weak oysters (slow shell-closing response) and four moribund oysters (no shell-closing response, but not yet undergoing liquefactive necrosis), were collected and preserved for DNA extraction during a mortality event on August 12. Each gill clipping was transferred from RNALater to a 1.7-ml microcentrifuge tube containing 500  $\mu\text{l}$  of lysis buffer (1-M Tris-HCl, pH 8.0; 0.5-M EDTA, pH 8.0; 1% sodium dodecyl sulfate) and ~30 mg of silica beads, and homogenized using a Mini Bead-beater (BioSpec Products, Bartlesville, OK, USA) for 30 s. Proteinase K (250  $\mu\text{g}$ ) was added to each sample, followed by incubation in a shaker incubator (Excella E24, New Brunswick Scientific, Edison, NJ, USA) for 16 h at  $37\text{ }^{\circ}\text{C}$  and 150 rpm. Chloroform:isoamyl alcohol (24:1, 500  $\mu\text{l}$ ) was subsequently added to each sample, vortexed for 1 min, and centrifuged at 14,000 g for 5 min. The upper aqueous phase was removed and placed in a clean microcentrifuge tube for DNA purification by ethanol precipitation. Ice-cold ethanol (100%, 400  $\mu\text{l}$ ) was added and samples were centrifuged at 14,000 g for 10 min. The supernatant was removed and the pellet washed with 200  $\mu\text{l}$  of ethanol (80%). The samples were centrifuged at 14,000 g for 10 min and the supernatant was removed. The pellet was air dried and re-suspended in 50  $\mu\text{l}$  of Tris EDTA buffer (10 mM Tris-HCl and 1 mM EDTA- $\text{Na}_2$ ).

## Microbial composition

A volume of 5  $\mu\text{l}$  (diluted to 25  $\text{ng } \mu\text{l}^{-1}$ ) from each oyster DNA sample was pooled across the four replicates for each density and time point during the experimental trial. Additionally, the weak-response oyster samples were pooled and the moribund oyster samples were pooled, for a total of 38 samples for high-throughput sequencing analysis of microbial communities. Amplicons of the V3 – V4 region of the 16S rRNA gene were generated by a nested PCR with two rounds of amplification, both using a 20- $\mu\text{l}$  reaction volume containing 10  $\mu\text{l}$  of 2X GoTaq Green Master Mix (Promega Corporation, Madison, WI, USA), 2  $\mu\text{l}$  of both forward and reverse primers (1  $\mu\text{M}$  final concentration), 1  $\mu\text{l}$  of template DNA, and 7  $\mu\text{l}$   $\text{dH}_2\text{O}$ , using a SimpliAmp Thermal Cycler (Thermo Fisher Scientific, Waltham, MA, USA). The first round of PCR used the primers F357 (5' TACGGGAGGCAGCAG) and R806 (5'GGACTACVSGGGTATCTAAT), with thermocycling settings of 95.0 °C hot start for 4 min, followed by 25 cycles of 95.0 °C for 30 s, 53.4 °C for 45 s, and 72.0 °C for 2 min, followed by a final elongation step for 5 min at 72.0 °C (Fisher et al. 2016). The second round of PCR used the forward primer F341, which included a variable Ion Xpress barcoded region (bold) and a sequencing adaptor (underlined and bold) (5' CCATCTCAT CCCTGCGTGTCTCCGACTCAGCTAAGGTAACGATTACGGGAGGCAGCAG 3') and the reverse primer 806R, which contained a P1 adaptor (underlined) (5' CCACTACGC CTCCGCTTTCTCTC TATGGGCAGTCGGTGATGG ACTACVSGGGTATCTAAT 3'). The thermocycling settings were 95.0 °C hot start for 4 min, followed by 20 cycles of 95 °C for 30 s, 65.0 °C for 45 s, and 72.0 °C for 2 min, followed by a final elongation step for 5 min at 72.0 °C. Following PCR amplification, each product was purified with the Agencourt AMPure XP magnetic bead cleanup protocol (Beckman Coulter, Inc., Brea, CA, USA), using a magnetic PCR plate rack, and quantified on a Qubit 2 Fluorometer using the Quant-iT dsDNA BR Assay Kit (Thermo Fisher Scientific).

Following purification of the second PCR products, barcoded amplicons from each sample were pooled at equimolar amounts and the library dilution factor was determined based on quantification with an Ion Library Quantitation Kit on an ABI QuantStudio 3 Real-Time PCR System (Applied Biosystems, Foster City, CA, USA). An Ion 520 and Ion 530 Kit-Chef on an Ion Chef Instrument was used to prepare DNA for sequencing, which was completed on an Ion 530 chip with 400 bp chemistry on an Ion S5 XL System (Life Technologies Inc., Carlsbad, CA, USA). Sequencing data were processed in Torrent Suite 5.10.0 with Pre-BaseCaller and BaseCaller Args set to disable-all-filters. The resulting multiplexed BAM (binary alignment and map) file was exported and passed to AMPtk v1.2.5 (Palmer et al. 2018) for de-multiplexing with the AMPtk ion script using default parameters (minimum read length 100 bases, trim all reads to 300 bases, no barcode mismatches, 2 base primer mismatch allowed, USEARCH v9.2.64, VSEARCH v2.9.0). Concatenated de-multiplexed data files were used for OTU clustering at 97% with AMPtk cluster and filtered with AMPtk filter. The taxonomic designation was assigned using the AMPtk taxonomy script and the AMPtk bacterial 16S database, prepared from rdp\_16S\_v16 from drive5 Bioinformatics Software and Services.

## Quantification of *Vibrio aestuarianus*

*Vibrio* spp., including *V. aestuarianus*, were isolated from local oysters as described in Cowan et al. (2023). The isolates were used to design species-specific *recA* primers and

probes for use in the detection and quantification of *V. aestuarianus*. Each 10- $\mu$ l qPCR reaction contained 5  $\mu$ l SSO Advanced Universal Probes Supermix (Bio-Rad, Hercules, CA, USA), 0.25  $\mu$ l of both forward (5'-AGGTTTCGATCATGCG CCTAG-3') and reverse (5'-CTGACGATTCCGGGCCATAG-3') primers, 0.1  $\mu$ l of probe (5'-[HEX] TACGATGGA TGTTGAAACCATCTCTACTG [BHQ1]-3'), 1.9  $\mu$ l of dH<sub>2</sub>O, and 2.5  $\mu$ l of extracted DNA from a sampled oyster at 25 ng  $\mu$ l<sup>-1</sup>. Reaction conditions included an initial denaturation phase of 5 min at 95 °C followed by 40 cycles of 15 s at 95 °C and 15 s at 60 °C. All samples were analyzed in duplicate in a 384-well, hard-shell PCR plate (Bio-Rad) on a CFX384 Real-Time System using the Bio-Rad CFX Maestro version 1.1 software (Bio-Rad). The standard curve was prepared through five tenfold dilutions of a known density of cultured *V. aestuarianus*. The RecA qPCR amplicons were Sanger sequenced in both directions (Eurofins MWG Operon Inc., Huntsville, AL, USA), a consensus sequence was aligned by ClustalW on MEGA10, and a basic local search tool analysis was conducted on the National Center for Biotechnology Information Sequence Database.

### Potentially harmful phytoplankton

Water samples (15 in total) were collected approximately weekly during the experiment for analysis of phytoplankton composition and biomass. One 15-m vertical tow, using a 20- $\mu$ m mesh plankton net, and one discrete water sample at 5-m depth, using a Van Dorn bottle, were taken at Metcalf Bay and stored in 125-ml bottles. The samples were preserved with a final concentration of 0.3 and 0.04% v/v Lugol's iodine solution, respectively. Potentially harmful algal species were identified, as identified by Cassis et al. (2011) and Nicky Haigh (Microthalassia Consultants Inc., pers. comm), and included *Alexandrium* spp., *Dictyocha speculum*, *Dinophysis* spp., *Heterosigma akashiwo*, *Protoceratium reticulatum*, *Pseudonitzschia* spp., and *Rhizosolenia setigera*. Identification of all phytoplankton taxa was done to the lowest practical taxonomic level, based on morphology (Hasle 1978), with a compound microscope using a Sedgewick-Rafter slide. The total phytoplankton abundance was subjectively scored on a qualitative scale from 1 to 5, which corresponds to a range of very low (1–2 cells ml<sup>-1</sup>) to very high (10,000 cells ml<sup>-1</sup>).

### Statistical analysis and visualization

All statistical analyses and visualizations were performed using the R statistical language (R Core 2020). Values in the present study are represented as mean  $\pm$  standard deviation unless otherwise indicated. Graphics were created using the packages ggplot2 (Wickham 2016) in R and Microsoft Excel 2016. To examine the density-dependent effects on oyster size, reproductive effort, and mortality, end values from each tray were compared with a linear mixed-effects regression (LMER), with density as a fixed factor and block as a random effect using the lme4 package (Bates et al. 2019). Pairwise comparisons were conducted using the Tukey HSD significance test in the emmeans package with  $\alpha=0.05$  (Lenth et al. 2020). The assumptions of normality and homoscedasticity for a linear model were confirmed by the Shapiro–Wilk test and Levene's test, respectively. Size and reproductive effort values were square-root transformed and final cumulative mortality was arcsine transformed to meet those assumptions.

The 16S rRNA gene OTUs were investigated using the Vegan package (Dixon 2003). The read number varied from 13 to 185,473. Seventeen samples below the threshold of 9150 reads based on the rarefaction curve were removed, and the remaining 21 samples

were rarefied to 9150 reads. Non-metric multidimensional scaling (NMDS) plots using Bray Curtis dissimilarity were generated for exploratory data analysis and a permutational multivariate analysis of variance (PERMANOVA) was used to examine statistical differences in microbial community composition between groups. Similarity percentage analysis (SIMPER) was used to further examine which OTUs contributed to the significant difference in microbial composition. The relationship between height, width, and length was examined by principal components analysis (PCA).

## Results

### Mortality

From May 11 to July 15 there was no observed mortality in any of the replicate trays (Fig. 2). Mortality was first noted on July 30 with  $10.75 \pm 1.97\%$  mortality across all densities, which coincided with a period of elevated temperature. Cumulative mortality measured on September 17 was  $52.9 \pm 11.8\%$  across all densities.

### Effects of stocking density

Cumulative mortality decreased with increased stocking densities, the highest stocking density having significantly lower mortality than the lowest one ( $p=0.023$ ) (Fig. 3). Density also had significant effects on oyster shell width ( $p=0.001$ ) and length ( $p=0.002$ ), with higher densities having significantly smaller oysters than lower ones (Fig. 4). Oyster shell height decreased with increasing stocking density, although the

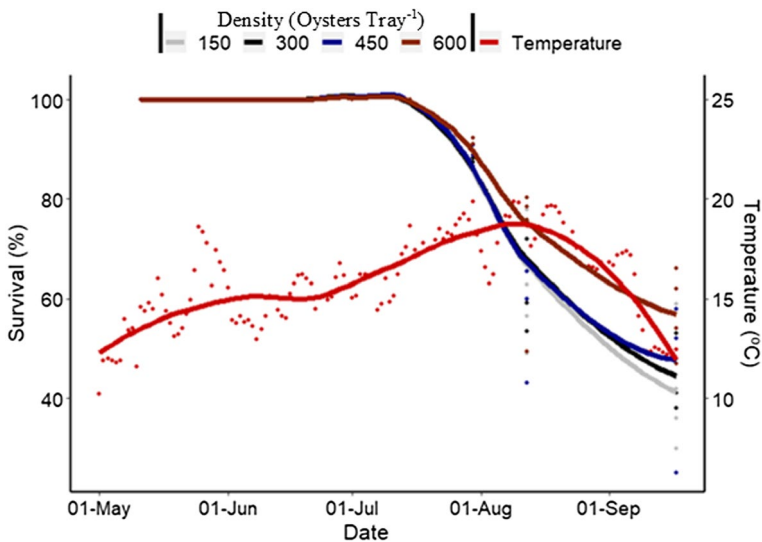


**Fig. 2** Percent oyster survival over time at four stocking densities (150, 300, 450, and 600 oysters tray<sup>-1</sup>). Daily water temperatures (red line) were acquired from DFO monitoring at Chrome Island lighthouse (DFO 2019). Fitted curves are smoothed conditional means using local polynomial regression fitting

**Fig. 3** Final mean  $\pm$  SE ( $n=4$ ) oyster cumulative mortality in the four oyster stocking densities (150, 300, 450, and 600 oysters tray<sup>-1</sup>). Significant differences among treatments are indicated ( $p < 0.05$ , Tukey HSD test)

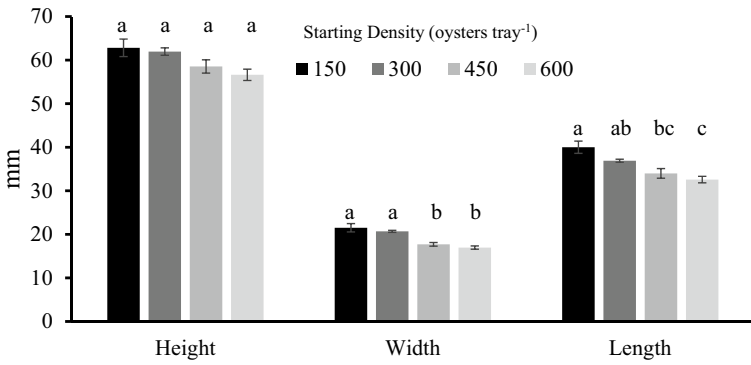
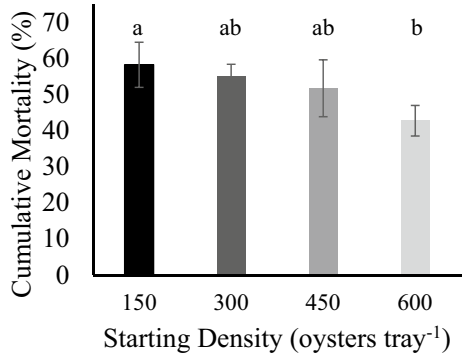


**Fig. 4** Final mean  $\pm$  SE ( $n=4$ ) oyster shell height, width, and length in the four oyster stocking densities (150, 300, 450, and 600 oysters tray<sup>-1</sup>). Significant differences among treatments are indicated ( $p < 0.05$ , Tukey HSD test)

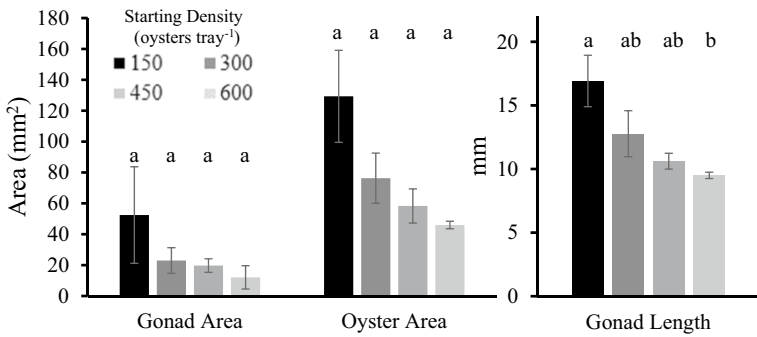


**Fig. 5** Final mean  $\pm$  SE ( $n=4$ ) oyster gonad area, oyster area, and gonad length in the four oyster stocking densities (150, 300, 450, and 600 oysters tray<sup>-1</sup>). Significant differences among treatments are indicated ( $p < 0.05$ , Tukey HSD test)

effect was marginally non-significant ( $p = 0.057$ ) (Fig. 4). Gonad length also decreased significantly with increasing density ( $p = 0.049$ ), the lowest and highest stocking densities being significantly different from one another (Fig. 5). Both gonad area and oyster

area also decreased with increasing stocking density, but the effects were non-significant ( $p=0.718$  and  $p=0.070$ , respectively) (Fig. 5).

## Growth and reproductive development

Throughout the experiment, the average shell height, width, and length of oysters across all trays and densities increased from  $14.2 \pm 0.5$ ,  $4.7 \pm 0.2$ , and  $11.0 \pm 0.3$  mm to  $60.0 \pm 0.9$ ,  $19.2 \pm 0.6$ , and  $35.9 \pm 0.9$  mm, respectively. The relationship between height, width, and length was examined by PCA, with PC1 describing 98.3% of the variation in those size measurements. Based on PC1, the oysters had an average 320.0% increase in shell size from May 11 to July 30 at the onset of the mortality event. Similarly, oyster reproductive development shifted from predominantly undifferentiated gonads (14/16 individuals) with 1 male and 1 female on May 23 to predominantly late active and ripe gonads (15/16 individuals) with 8 males and 8 females on July 30 at the onset of the mortality event. Over the same period, a change in gonad area from  $0.04 \pm 0.14$  to  $14.49 \pm 12.79$  mm<sup>2</sup> was observed and the gonadosomatic index increased from  $0.48 \pm 1.66$  to  $24.23 \pm 11.90\%$  gonad occupation. A PCA of reproductive effort assessed the correlation between developmental stage, gonad area, gonad length, and gonadosomatic index, PC1 describing 79.4% of the variation in reproductive effort (Fig. 6). Throughout the period of observation, there was a linear relationship between log-transformed values of oyster size (PC1) and values of reproductive development (PC1) ( $R^2=0.652$ ,  $p<0.00001$ ).

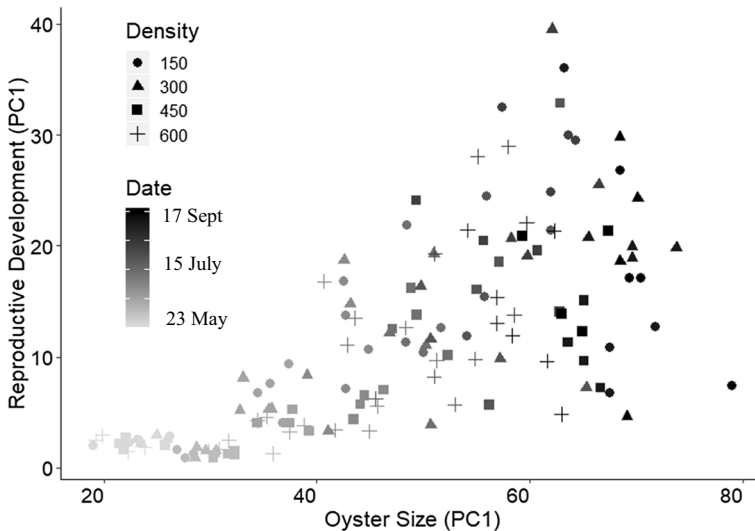


**Fig. 6** Each point represents a replicate tray containing 150, 300, 450, or 600 Pacific oysters. Principal component (PC) 1 of oyster size variables described 98.3% of the variation in shell height, width, and length. PC1 of oyster reproductive development described 79.4% of variation in oyster gonad length, gonad area, gonadosomatic index, and gonad developmental phase

## Environmental observations

The YSI-EXO2 sonde, located at Fanny Bay, recorded data from May 11 to August 2. The average daily temperature was  $15.7 \pm 2.0$  °C (min: 11.0 °C, max: 18.9 °C), oxygen saturation was  $114.1 \pm 11.3\%$  (min: 91.0%, max: 143.4%), salinity was  $26.2 \pm 1.1$  ppt. (min: 23.3 ppt, max: 28.0 ppt), chlorophyll was  $35.37 \pm 64.13$   $\mu\text{g l}^{-1}$  (min: 0.15  $\mu\text{g l}^{-1}$ , max: 317.5  $\mu\text{g l}^{-1}$ ), and turbidity was  $5.26 \pm 9.67$  formazin nephelometric units (fnu) (min: 0.06 fnu, max: 49.3 fnu). Eleven surface carbonate chemistry samples were collected at Metcalf Bay from July 18 to September 18. The pH,  $\text{pCO}_2$ , and aragonite saturation throughout the study was  $8.17 \pm 0.02$  (min: 8.1, max: 8.3),  $258.5 \pm 15.7$   $\mu\text{ATM}$  (min: 167.0  $\mu\text{ATM}$ , max: 349.0  $\mu\text{ATM}$ ), and  $2.34 \pm 0.10$  (min: 1.96, max: 2.95), respectively. Throughout the experiment, the daily average temperature recorded by the HOBO® pendants at 5-m depth was  $16.1 \pm 2.0$  °C (min: 11.0 °C, max: 19.9 °C) whereas the daily average temperature on the 10 days preceding the first observed mortality, from July 21 to July 30, was  $18.7 \pm 0.6$  °C (min: 16.6 °C, max: 19.9 °C). Those daily temperature averages derived from HOBO® deployments, recorded at 10-min intervals, had a strong correlation with the single daily temperature sample from the Chrome Island lighthouse ( $R^2=0.88$ ). The Chrome Island data provide a historic context for the recorded temperatures, with the 5 days preceding the onset of the mortality event exceeding the 80th percentile for the last 30 years for their respective dates.

## Necropsy and histological observations

No macroscopic lesions or abnormalities were observed in any of the 144 oysters sampled for histopathology and no pathologies from pathogens of regional concern (Bower 2017) were detected via histological examination. However, irregularly shaped microcolonies of Rickettsia-like organisms were observed within the stomach epithelium of one specimen that was collected on August 12 (Supp. Fig. 2). In addition, three of 16 specimens collected on August 12 (during the mortality event) displayed necrosis in the gills and other peripheral tissues that was associated with the presence of mixed types of bacteria (Fig. 7). Those samples had the highest proportion of OTU1 in 16 s rRNA amplicon sequencing and the highest abundance of *V. aestuarianus* in qPCR analysis.

## 16S rRNA Amplicon Sequencing

A total of 1056 OTUs were present and the average per sample was  $310.6 \pm 111.0$  OTUs. Of the 1056 OTUs, 983 were identified to class and 340 to genus. The most common classes were Gammaproteobacteria (310 OTUs), Alphaproteobacteria (165), Flavobacteria (89), and Deltaproteobacteria (84), while the most common genera were *Arcobacter* (17 OTUs), *Vibrio* (11), and *Psychromonas* (8). Eight of the most abundant OTUs, primarily of the genera *Vibrio*, *Serratia*, *Pseudomonas*, and *Psychromonas*, made up 48.6% of the read counts across all samples (Fig. 8).

The NMDS of Bray Curtis dissimilarity clustered by density (not shown) revealed that there was no significant difference in microbial composition based on stocking density, a result that was supported by the PERMANOVA ( $p=0.599$ ,  $R^2=0.156$ ). There was, however, a significant difference ( $p=0.009$ ,  $R^2=0.349$ ) in bacterial composition among groups of samples associated with observed low ( $<0.1\% \text{ d}^{-1}$ ), medium ( $0.1\text{--}2\% \text{ d}^{-1}$ ), and high ( $>2\% \text{ d}^{-1}$ ) percent mortalities (Supp. Fig. 3). The PERMANOVA analysis

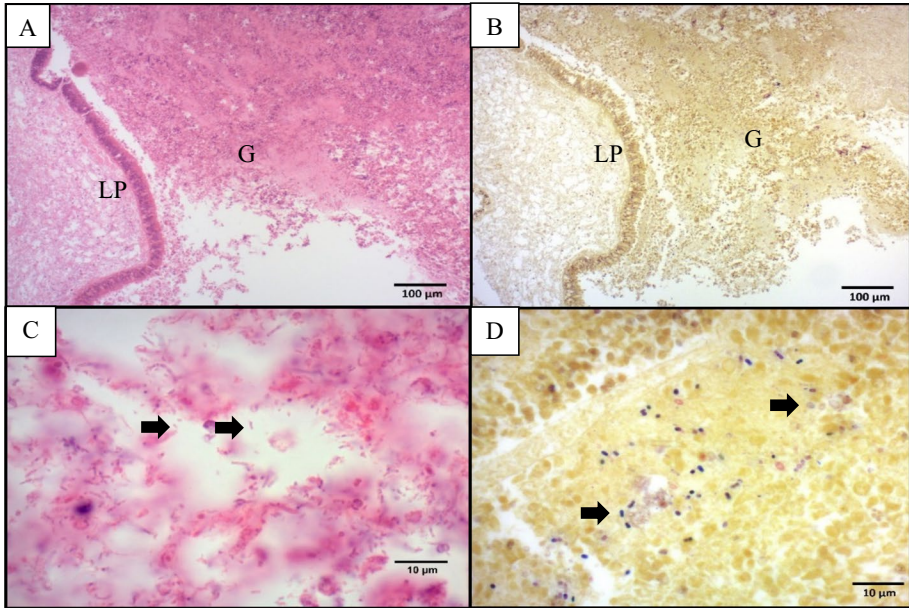


**Fig. 7** Histological tissue sections of a Pacific oyster that appeared healthy macroscopically that was collected on August 12 during the mortality event. Figures **A** and **C** stained with H&E and figures **B** and **D** stained with Gram stain. Figures **A** and **B** are low magnification showing healthy labial palps (LP) adjacent to necrotic gill tissue (G). Figures **C** and **D** are high magnifications of the necrotic gill tissue showing mixed bacterial infections (arrows) that are more easily discerned with Gram stain

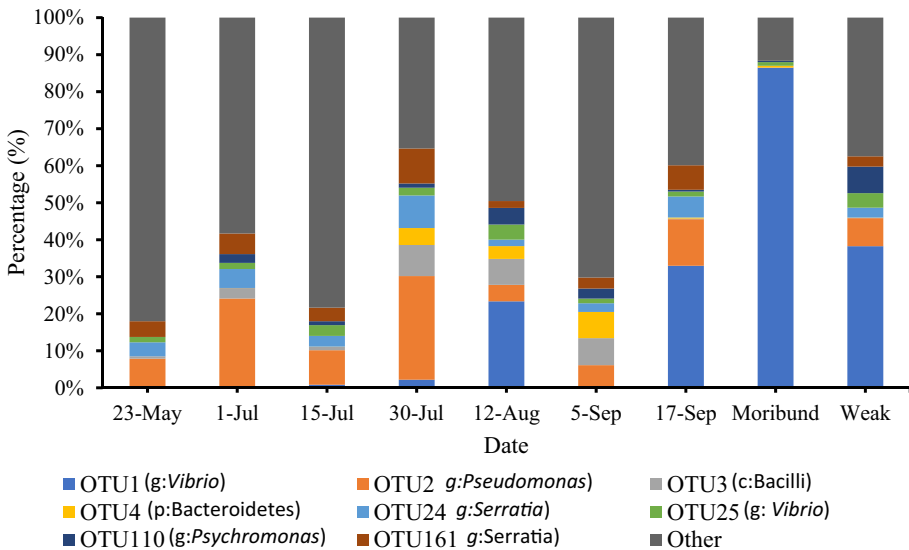


**Fig. 8** Stacked bar plot of Pacific oyster bacterial microbiome. Shown identities are the nearest result from the AMPTk v1.2.5 16S rRNA gene database (Palmer et al. 2018) using AMPTk taxonomy with 97% nucleotide clustering. Data pooled across all density treatments

suggests that there was a significant difference between the low and medium mortality groups ( $p=0.003$ ,  $R^2=0.169$ ) and the low and high ones ( $p=0.012$ ,  $R^2=0.244$ ), but not between the medium and high mortality groups ( $p=0.079$ ,  $R^2=0.172$ ). The variation between clusters of samples from low, medium, and high mortality groups was driven predominantly by OTU1. For example, OTU1 explained 36.0% of the variation among samples that appeared healthy and the combined weak and moribund samples in the PERMANOVA ( $p=0.028$ ,  $R^2=0.111$ ). In addition, OTU1 shared 99.7% nucleotide similarity with several *Vibrio* spp. including *V. aestuarianus* (GenBank: [KY923252.1](#)) (Saulnier et al. 2017).

### Quantification of *Vibrio aestuarianus*

Twenty-four of 144 samples were above the limit of detection of  $1.78 \log_{10}$  cells  $\text{ng}^{-1}$  of DNA (Fig. 9) and the standard curve had an  $R^2$  of 0.991 and an amplification efficiency of 1.006 ( $y = -3.308x + 44.388$ ). The concentration of *V. aestuarianus* was highest in moribund oysters and was elevated during periods of observed mortality from July 30 to September 17. The qPCR product had a 99.3% nucleotide similarity with *V. aestuarianus* (GenBank: [AJ580855.1](#)) and 90.9% similarity to the next closest match, *V. scophthalmi* (GenBank: [CP016307.1](#)).

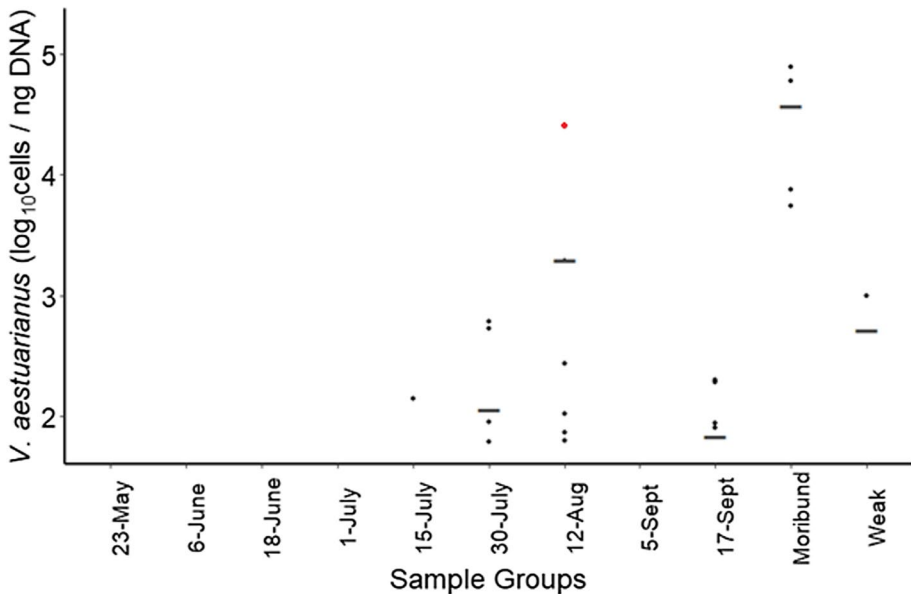


**Fig. 9** Quantitative polymerase chain reaction results for the detection of *Vibrio aestuarianus* in Pacific oyster gill tissue samples. Sixteen samples were collected from oysters that appeared healthy macroscopically per week and the group averages are shown with black bars. Four moribund and two weak individuals were collected during the mortality event on August 12, 2018. The red dot is the same oyster with a mixed microbial infection shown in Fig. 7

## Phytoplankton

*Rhizosolenia setigera* was the most abundant potentially harmful (Nicky Haigh, Microthalassia Consultants Inc., pers. comm.) phytoplankton species present in the upper water column in Baynes Sound in the summer of 2018, with an average of 233.5 cells ml<sup>-1</sup> across all samples (Fig. 10). Other prevalent, potentially harmful phytoplankton species included *Pseudonitzschia pungens*-type (69.4 cells ml<sup>-1</sup>), *Eucampia zodiacus* (17.9 cells ml<sup>-1</sup>), and *H. akashiwo* (1.5 cells ml<sup>-1</sup>). The average concentration of the total phytoplankton community collected during the experimental was 3500 ± 1000 cells ml<sup>-1</sup>.

## Discussion

### Summary of observed mortality

Water temperatures increased rapidly to over 19 °C at the end of July in Baynes Sound, which coincided with the onset of Pacific oyster mortalities in our study. Mortalities of the cultured oysters occurred during a period of rapid growth, with an increase in shell size of 320% between May 11 and July 30. Gametogenesis occurred simultaneously, most oysters developing gonads between May 23 and July 30. The correlation of Pacific oyster growth and reproductive development with their susceptibility to summer mortality and infection by opportunistic pathogens has been previously described (e.g., Cotter et al. 2010; De Decker et al. 2011; Wendling and Wegner 2013). The observed accumulation of *V. aestuarianus* and OTU1 in the gills during the mortality event was, therefore, likely a result of increased proliferation of bacteria, including pathogenic species, higher water temperatures, and increased host susceptibility to infection associated with elevated temperature, rapid host growth, and the onset of gametogenesis.

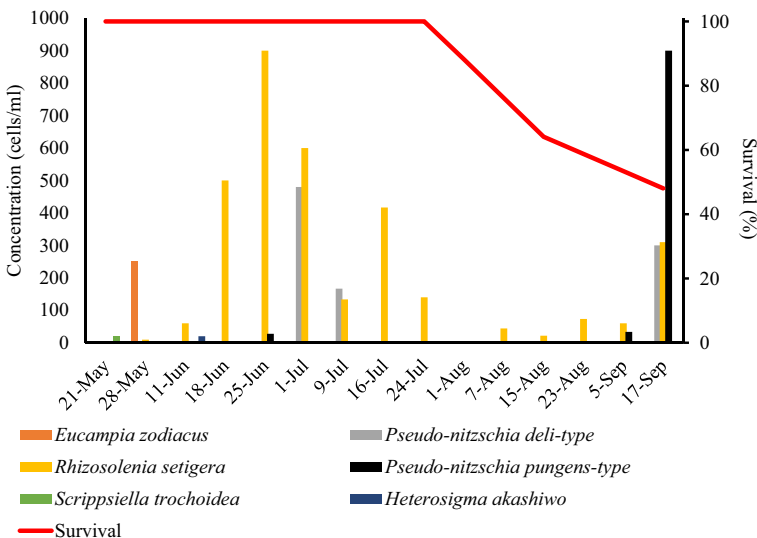


**Fig. 10** Concentrations of the most abundant phytoplankton species at 5-m depth in Metcalf Bay. The red line is percent survival of the oysters

## Environmental data and harmful algal species

Environmental characteristics can play a critical role in Pacific oyster summer mortality (King et al. 2019a). Our observed values and associated variations of carbonate chemistry, oxygen, chlorophyll, salinity, and turbidity were all within the optimal range for promoting Pacific oyster growth. The water temperatures increased rapidly from early July to mid-August, the former date coinciding with the onset of mortalities (Fig. 2). Elevated temperatures can increase the proliferation and virulence of pathogens while simultaneously increasing physiological stress, impaired immune responses, and susceptibility of the hosts (Malham et al. 2009; Kimes et al. 2012; Wendling et al. 2014; Barbosa-Solomieu et al. 2015).

Among the taxa of potentially harmful algal species observed in the present study, there is limited evidence of cumulative impacts associated with disease susceptibility or reduced oyster fitness. Keppler et al. (2005) and Abi-Khalil et al. (2016) considered that *H. akashiwo* and *Alexandrium* spp. were harmful phytoplankton taxa that may have contributed to cumulative stress and mortalities of oysters. However, laboratory experiments suggest both increased disease susceptibility and sublethal effects occur in oysters when phytoplankton concentrations are 10,000 and 1000 times greater than the observed concentrations in the present study for *H. akashiwo* and *Alexandrium* spp., respectively (Keppler et al. 2005; Abi-Khalil et al. 2016). Further, flagellate diel migration in situ would lessen the harmful exposure relative to laboratory-based, constant exposure conditions. However, it should be noted that the causes of summer mortality can vary across time and space and, while not seeming to be important in the present work, harmful algae could be involved in some cases of oyster summer mortality.

## Effect of stocking density

In our study, there was a negative relationship between starting stocking densities and size, reproductive effort, and mortality of oysters. That contrasts with Chávez-Villalba et al. (2010) who did not observe a significant effect of stocking density on Pacific oyster survival in Mexico. Their densities (ranging from 7.6 to 181.5 oysters  $m^{-2}$ ), however, were somewhat lower compared to those in the present work (71.4 to 285.6 oysters  $m^{-2}$ ). As in our study, they observed lower oyster growth at the highest stocking density; however, they did not quantify or characterize factors related to gametogenesis or reproductive effort (Chávez-Villalba et al. 2010). Additionally, their study was conducted in a subtropical lagoon, where they observed many months that exceeded the maximum average daily temperature observed in our study. Field observations suggest reducing food availability with higher stocking densities will reduce gonad development (Royer et al. 2008; Chávez-Villalba et al. 2010). Combined, those field studies provide evidence that limiting food availability may indirectly reduce mortalities through a reduction in oyster growth and reproductive effort. Controlled laboratory studies on food availability have yielded comparable results with increased food availability causing significantly higher summer mortalities (Lipovsky and Chew 1972; Delaporte et al. 2007; Malham et al. 2009). The observed effect of stocking density on survival in our study suggests that higher densities in the summer could be an effective and easily implementable method for farmers to mitigate the extent of summer mortalities.

## Histology and microbial analysis

Histological examination of oyster cross sections did not reveal the presence of any pathologies of regional concern (Bower 2017). Micro-colonies of Rickettsia-like organisms were observed within the stomach epithelium of one specimen; however, there was no associated host response or pathology. Furthermore, infections with that bacterium have not been implicated in previously published investigations concerning the cause of summer mortality of Pacific oysters. Three of 16 specimens collected on August 12 (during the mortality event) displayed necrosis of the gills and other peripheral tissues that were associated with a mixed microbial infection. The gram stain showed an abundance of gram-positive and gram-negative bacteria within the necrotic tissues.

During the observed period of mortalities in the present study, the abundance and relative proportion of *V. aestuarianus* increased in healthy, weakened, and moribund oyster samples. *Vibrio aestuarianus* was first isolated from seawater, clams, oysters, and crabs along the Oregon coast and later reported as a pathogen of Pacific oysters in France (Tison and Seidler 1983; Labreuche et al. 2006a). Following the association of *V. aestuarianus* with Pacific oyster summer mortality in France (Garnier et al. 2007), it was split into two sub-species, *V. aestuarianus* subsp. *aestuarianus* (Tison and Seidler 1983) and *V. aestuarianus* subsp. *francensis* (Garnier et al. 2008). Due to the significance of Pacific oyster summer mortality in France, *V. aestuarianus* subsp. *francensis* has been well-studied (e.g., Labreuche et al. 2006b, 2010; Parizadeh et al. 2018). Like most pathogenic *Vibrio* spp., the virulence of *V. aestuarianus* to Pacific oysters is strain-dependent (Garnier et al. 2008; Baker-Austin et al. 2018). Investigations into a highly pathogenic strain of *V. aestuarianus* subsp. *francensis* (01/32) revealed an extracellular zinc metalloprotease that confers the cytotoxicity and virulence (Labreuche et al. 2006a, b, 2010). This metalloprotease induces morphological changes in oyster hemocytes, causing reduced function and survival, leading to host immunosuppression.

At a temperature of 5 °C, *V. aestuarianus* can be present in oysters at concentrations below the detectable limits, but is detectable following thermal stress (Parizadeh et al. 2018). That observation suggests that *V. aestuarianus* may have been present in oysters throughout May and June, at concentrations below the qPCR limit of detection, and did not proliferate until more favorable environmental and physiological conditions supported its rapid growth. Lokmer and Wegner (2015) demonstrated that the composition and abundance of OTUs in healthy Pacific oyster microbiomes change significantly with temperature treatments, but not from a challenge with a virulent *Vibrio* sp. Similarly, a study with a simulated marine heatwave of  $\Delta 5$  °C over 6 days resulted in a cumulative Pacific oyster mortality of 77.4%, a reduction in microbial diversity, and a 324-fold increase in *V. harveyi* concentration (Green et al. 2019).

It is currently unknown if *V. aestuarianus* in Baynes Sound is an opportunistic pathogen that can grow rapidly as a secondary infection or a causative mechanism in observed Pacific oyster summer mortalities. Future work should characterize the virulence of *V. aestuarianus* through controlled laboratory challenges of Pacific oysters with strains isolated from this area.

## Growth and reproductive effort

This study provides evidence for the association of reproductive effort with summer mortality. Such a link has been observed in field studies conducted in other parts of the world (Imai et al. 1965; Lipovsky and Chew 1972; Perdue 1983; Cotter et al. 2010) as well as in laboratory trials (Delaporte et al. 2007; Huvet et al. 2010; Wendling and Wegner 2013), but not in cultivated oysters in coastal waters of BC. At the onset of summer mortality on July 30, we observed a gonadosomatic index of 24%, whereas during the anomalously warm period in May, the oysters had a GSI of only 0.48%. Many summer mortality studies have focused on Pacific oysters in their second summer when they typically have a much higher GSI (e.g., Perdue 1983; Azéma et al. 2016). Mature gametes in Pacific oysters are associated with oyster size, not age, and the amount of reproductive effort is a product of food availability (Quayle 1988; Enríquez-Díaz et al. 2009). In addition, there is evidence that the proportion of female oysters is positively correlated with food supply and oyster age (Quayle 1988; Cowan et al. 2023). Pacific oysters are protandrous hermaphrodites and are thought to be all males during their first summer of reproductive development (Pauley et al. 1988). In contrast, in the present study, a substantial proportion of oysters (e.g., 50% on July 30) were female throughout their first summer. The mechanism by which gametogenesis could increase susceptibility to summer mortality is not well understood (De Decker et al. 2011). The process of gametogenesis may directly lower the immune response of oysters by reducing the number of circulating hemocytes (Delaporte et al. 2006). De Decker et al. (2011) also observed that *V. splendidus* preferentially infects gonad tissue, however, we detected only *V. aestuarianus* in gill epithelium.

Despite the correlations in occurrence of gametogenesis and summer mortality in field and laboratory studies, there is little evidence that triploid oysters with reduced reproductive capacity experience lower summer mortalities. Triploid oysters are often considered partially sterile, with approximately 0.06% of the reproductive potential of diploid oysters (Allen and Downing 1986; Suquet et al. 2016; Houssin et al. 2019). Their gonadosomatic index is also significantly lower than that of diploids (Jeung et al. 2016). Suquet et al. (2016) observed gametes in 92.9% of diploid oysters and in only 42.0% of triploid individuals. Despite their reduced reproductive effort, Wadsworth et al. (2019) observed significantly higher summer mortalities in triploid Eastern oysters (*Crassostrea virginica*) compared with diploids. Comparative studies of diploid and triploid Pacific oysters may present an opportunity for the differential examination of the role of reproductive effort and energy utilization in summer mortality (Allen and Downing 1986).

## Conclusions

The present study demonstrated that summer mortalities of  $52.9 \pm 11.8\%$  can occur during the first summer of growth of Pacific oysters in suspended culture in Baynes Sound. We demonstrated that increased *V. aestuarianus* abundance, elevated water temperatures, and rapid growth/gametogenesis are associated with summer mortalities in the region. The effect of stocking density on mortality suggests that reducing food availability may alter Pacific oyster susceptibility to summer mortality. An improved understanding of oyster energetics during periods of gametogenesis may identify improved management strategies for oyster farmers in the region.

**Supplementary Information** The online version contains supplementary material available at <https://doi.org/10.1007/s10499-024-01415-5>.

**Acknowledgements** We thank Mac's Oysters Ltd. and their staff for their invaluable support, Jessica Driver, Daniel Roth, and Emily Warren for their contributions to field work and sample preparation, and Alexa McMillan for her assistance in the laboratory. The project was funded by the Aquaculture Collaborative Research and Development Program of Fisheries and Oceans Canada and by Mac's Oysters Ltd.

**Author contribution** (A) M.W. Cowan, (B) C.M. Pearce, (C) T.J. Green, (D) T. Finston, (E) G.R. Meyer, (F) B. McAmmond, (G) J.D. Van Hamme, (H) E.M. Bottos, (I) R. Marshall, (J) W. Evans, (K) T.F. Sutherland, (L) P.Y. de la Bastide.

B, I wrote funding proposal and secured funding.

B, C, D, E, G, H, J, K, L provided laboratory space and equipment.

A, E, F, K did the experimental work.

A, B, C, D, E, F, G, H, J, K, L contributed to the data analysis.

A wrote the main manuscript text.

All authors reviewed the manuscript.

**Funding** Open Access funding provided by Fisheries & Oceans Canada. This project was funded by the Aquaculture Collaborative Research and Development Program of Fisheries and Oceans Canada (project number: 17-P-05) and by Mac's Oysters Ltd.

**Data availability** Data are available upon request to the lead author (CMP).

## Declarations

**Ethical approval** All animal research was approved by Fisheries and Oceans Canada's Pacific Region Animal Care Committee.

**Competing interests** The authors declare no competing interests.

**Open Access** This article is licensed under a Creative Commons Attribution 4.0 International License, which permits use, sharing, adaptation, distribution and reproduction in any medium or format, as long as you give appropriate credit to the original author(s) and the source, provide a link to the Creative Commons licence, and indicate if changes were made. The images or other third party material in this article are included in the article's Creative Commons licence, unless indicated otherwise in a credit line to the material. If material is not included in the article's Creative Commons licence and your intended use is not permitted by statutory regulation or exceeds the permitted use, you will need to obtain permission directly from the copyright holder. To view a copy of this licence, visit <http://creativecommons.org/licenses/by/4.0/>.

## References

- Abi-Khalil C, Lopez-Joven C, Abadie E, Savar V, Amzil Z, Laabir M, Rolland J (2016) Exposure to the paralytic shellfish toxin producer *Alexandrium catenella* increases the susceptibility of the oyster *Crassostrea gigas* to pathogenic *Vibrios*. *Toxins* 8:1–24. <https://doi.org/10.3390/toxins8010024>
- Allen SK, Downing LE (1986) Performance of triploid Pacific oysters, *Crassostrea gigas* (Thunberg). I. Survival, growth, glycogen content, and sexual maturation in yearlings. *J Exp Mar Biol Ecol* 102:197–208. [https://doi.org/10.1016/0022-0981\(86\)90176-0](https://doi.org/10.1016/0022-0981(86)90176-0)
- Azéma P, Travers M, Benabdelmouna A, Dégremont L (2016) Single or dual experimental infections with *Vibrio aestuarianus* and OsHV-1 in diploid and triploid *Crassostrea gigas* at the spat, juvenile and adult stages. *J Invertebr Pathol* 139:92–101. <https://doi.org/10.1016/j.jip.2016.08.002>
- Baker-Austin C, Oliver JD, Alam M, Ali A, Waldor MK, Qadri F, Martinez-Urtaza J (2018) *Vibrio* spp. infections. *Nat Rev Dis Primers* 2:1–19. <https://doi.org/10.1038/s41572-018-0005-8>
- Barbosa-Solomieu VB, Renault T, Travers M (2015) Mass mortality in bivalves and the intricate case of the Pacific oyster, *Crassostrea gigas*. *J Invertebr Pathol* 131:2–10. <https://doi.org/10.1016/j.jip.2015.07.011>

- Bates D, Maechler M, Bolker B, Walker S (2019) Fitting linear mixed-effects models using lme4. *J Stat Softw* 67:1–48. <https://doi.org/10.18637/jss.v067.i01>
- Bendell L (2019) Baynes Sound; its unique nature and the need to recognize the region as a marine protected area. Chapter 4 in *Stewarding the sound: the challenge of managing sensitive coastal ecosystems*. Eds: Bendell, L., Gallagher, P., McKeachie, S., Wood, L. CRC Press, Taylor, and Francis Group, Boca Raton, FL. <https://doi.org/10.1201/9780429025303>.
- Bower S (2017) Synopsis of infectious diseases and parasites of commercially exploited shellfish. Fisheries and Oceans Canada. Downloaded on March 3, 2020 from <http://www.dfo-mpo.gc.ca/science/aah-saa/diseases-maladies/toc-eng.html#oys>.
- Cassis D, Pearce CM, Maldonado MT (2011) Effects of the environment and culture depth on growth and mortality in juvenile Pacific oysters in the Strait of Georgia, British Columbia. *Aquac Environ Interact* 1:259–274. <https://doi.org/10.3354/aei00025>
- Chávez-Villalba J, Arreola-Lizárraga A, Burrola-Sánchez S, Hoyos-Chairez F (2010) Growth, condition, and survival of the Pacific oyster *Crassostrea gigas* cultivated within and outside a subtropical lagoon. *Aquaculture* 300:128–136. <https://doi.org/10.1016/j.aquaculture.2010.01.012>
- Cotter E, Malham SK, O'Keefe S, Lynch SA, Latchford JW, King JW, Beaumont AR, Culloty SC (2010) Summer mortality of the Pacific oyster, *Crassostrea gigas*, in the Irish Sea: the influence of growth, biochemistry and gametogenesis. *Aquaculture* 303:8–21. <https://doi.org/10.1016/j.aquaculture.2010.02.030>
- Cowan MW, Pearce CM, Finston T, Meyer GR, Marshall R, Evans W, Sutherland TF, de la Bastide PY (2023) Role of the *Vibrio* community, reproductive effort, and environmental parameters in intertidal Pacific oyster summer mortality in British Columbia, Canada. *Aquaculture* 565:739094. <https://doi.org/10.1016/j.aquaculture.2022.739094>
- De Decker S, Normand J, Saulnier N, Pernet F, Castagnet S, Boudry P (2011) Response of diploid and triploid Pacific oysters *Crassostrea gigas* to *Vibrio* infections in relation to their reproductive status. *J Invertebr Pathol* 106:179–191. <https://doi.org/10.1016/j.jip.2010.09.003>
- Delaporte M, Soudant P, Lambert C, Moal J, Pouvreau S, Samain J (2006) Impact of food availability on energy storage and defense related hemocyte parameters of the Pacific oyster *Crassostrea gigas* during an experimental reproductive cycle. *Aquaculture* 254:571–582. <https://doi.org/10.1016/j.aquaculture.2005.10.006>
- Delaporte M, Philippe S, Lambert C, Jegaden M, Moal J, Pouvreau S, Dégremont L, Boudry P, Samain J (2007) Characterisation of physiological and immunological differences between Pacific oysters (*Crassostrea gigas*) genetically selected for high or low survival to summer mortalities and fed different rations under controlled conditions. *J Exp Mar Biol Ecol* 353:45–57. <https://doi.org/10.1016/j.jembe.2007.09.003>
- DFO (2013) Socio-economic impact of aquaculture in Canada. Department of Fisheries and Oceans, Canada. Downloaded on March 2, 2020 from <https://www.dfo-mpo.gc.ca/aquaculture/sector-secteur/socio/index-eng.htm>.
- DFO (2019) British Columbia lightstgation sea surface temperature and salinity data (Pacific), 1914–present. Department of Fisheries and Oceans, Canada. Downloaded on March 3, 2020 from <https://open.canada.ca/data/en/dataset/719955f2-bf8e-44f7-bc26-6bd623e82884>.
- Dixon P (2003) VEGAN, a package of R functions for community ecology. *J Veg Sci* 14:927–930. <https://doi.org/10.1111/j.1654-1103.2003.tb02228.x>
- Elston RA, Beattie JH, Friedman C, Hedrick R, Kent ML (1987) Pathology and significance of fatal inflammatory bacteraemia in the Pacific oyster, *Crassostrea gigas* Thünberg. *J Fish Dis* 10:121–132. <https://doi.org/10.1111/j.1365-2761.1987.tb00727.x>
- Enríquez-Díaz M, Pouvreau S, Chávez-Villalba J, Le Pennec M (2009) Gametogenesis, reproductive investment, and spawning behaviour of the Pacific giant oyster *Crassostrea gigas*: evidence of an environment-dependent strategy. *Aquac Int* 17:491–506. <https://doi.org/10.1007/s10499-008-9219-1>
- Evans W, Pocock K, Hare A, Weekes C, Hales B, Jackson J, Gurney-Smith H, Mathis JT, Alin SR, Feely RF (2019) Marine CO<sub>2</sub> patterns in the northern Salish Sea. *Front Mar Sci* 5:536. <https://doi.org/10.3389/fmars.2018.00536>
- FAO (2018) FishStatJ statistics. Fisheries and Aquaculture Department, Food and Agriculture Organization of the United Nations. Downloaded on March 3, 2020 from <http://www.fao.org/fishery/statistics/en>.
- Fisher MA, Güllert S, Neulinger SC, Streit WR, Schmitz RA (2016) Evaluation of 16S rRNA gene primer pairs for monitoring microbial community structures showed high reproducibility within and low comparability between datasets generated with multiple archaeal and bacterial primer pairs. *Front Microbiol* 7:1297. <https://doi.org/10.3389/fmicb.2016.01297>
- Friedman CS, Hendrick RP (1991) Pacific oyster nocardiosis: isolation of the bacterium and induction of laboratory infections. *J Invertebr Pathol* 57:109–120. [https://doi.org/10.1016/0022-2011\(91\)90047-T](https://doi.org/10.1016/0022-2011(91)90047-T)

- Friedman CS, Beattie JH, Elston RA, Hendrick RP (1991) Investigation of the relationship between the presence of a gram-positive bacterial infection and summer mortality of the Pacific oyster, *Crassostrea gigas* Thunberg. *Aquaculture* 94:1–15. [https://doi.org/10.1016/0044-8486\(91\)90124-P](https://doi.org/10.1016/0044-8486(91)90124-P)
- Galstoff PS (1964) Morphology and structure of shell. Chapter 2 in *The American Oyster Crassostrea virginica* Gmelin. *Fishery Bulletin*, 64, 2. Downloaded on March 4, 2020 from <https://www.nefsc.noaa.gov/publications/classics/galtsoff1964/galtsoff1964.pdf>
- Garnier M, Labreuche Y, Garcia C, Robert M, Nicolas JL (2007) Evidence for the involvement of pathogenic bacteria in summer mortalities of the Pacific oyster, *Crassostrea gigas*. *Microb Ecol* 53:187–196. <https://doi.org/10.1007/s00248-006-9061-9>
- Garnier M, Labreuche Y, Nicolas J (2008) Molecular and phenotypic characterization of *Vibrio aestuarianus* subsp. *francensis* subsp. nov., a pathogen of the oyster *Crassostrea gigas*. *Syst Appl Microbiol* 31:358–365. <https://doi.org/10.1016/j.syapm.2008.06.003>
- Green TJ, Siboni N, King WL, Labbate M, Seymour JR, Raftos D (2019) Simulated marine heat wave alters abundance and structure of *Vibrio* populations associated with the Pacific oyster resulting in a mass mortality event. *Microb Ecol* 77:736–747. <https://doi.org/10.1007/s00248-018-1242-9>
- Hales B, Chipman D, Takahashi T (2004) High-frequency measurement of partial pressure and total concentration of carbon dioxide in seawater using microporous hydrophobic membrane contactors. *Limnol Oceanogr Methods* 2:356–364. <https://doi.org/10.4319/lom.2004.2.356>
- Hasle GR (1978) Identification problems. General recommendations. In: Sournia, A. (Ed.), *Phytoplankton manual*. Monographs on oceanographic methodology. UNESCO Publishing, 6, 135–128. Downloaded on March 3, 2020 from <https://unesdoc.unesco.org/ark:/48223/pf0000030788>.
- Houssin M, Trancart S, Denechere L, Oden E, Adeline B, Lepoitevin M, Pitel P (2019) Abnormal mortality of triploid adult Pacific oysters: is there a correlation with high gametogenesis in Normandy, France? *Aquaculture* 505:63–71. <https://doi.org/10.1016/j.aquaculture.2019.02.043>
- Howard DW, Lewis EJ, Keller BJ, Smith CS (2004) Histological techniques for marine bivalve molluscs and crustaceans. NOAA Technical Memorandum NOS NCCOS, 5, 218. Downloaded on March 3, 2020 from <https://nefsc.noaa.gov/nefsc/publications/tm/pdfs/tmfnc25.pdf>
- Huvet A, Normand J, Fleury E, Quillen V, Fabioux C, Bourdy P (2010) Reproductive effort of Pacific oysters: a trait associated with susceptibility to summer mortality. *Aquaculture* 304:95–99. <https://doi.org/10.1016/j.aquaculture.2010.03.022>
- Imai T, Kenichi N, Juichi O, Shigeru S (1965) The search for the cause of mass mortality and the possibility of its prevention by transplantation experiments. *Bull Tohokoku Reg Fish Res Lab* 25:27–38
- Jesser KJ, Noble RT (2018) *Vibrio* ecology in the Neuse River estuary, North Carolina characterized by next-generation amplicon sequencing of the gene ending heat shock protein 60 (*hsp60*). *Appl Environ Microbiol* 18:e00333–e418. <https://doi.org/10.1016/10.1128/AEM.00333-18>
- Jeung H, Keshavmurthy S, Lim H, Kim S, Choi K (2016) Quantification of reproductive effort of the triploid Pacific oyster, *Crassostrea gigas* raised in intertidal rack and bag oyster culture system off the west coast of Korea during spawning season. *Aquaculture* 464:374–380. <https://doi.org/10.1016/j.aquaculture.2016.07.010>
- Kamada N, Chen GY, Inohara N, Núñez G (2013) Control of pathogens and pathobionts by the gut microbiota. *Nat Immunol* 14:685–690. <https://doi.org/10.1038/ni.2608>
- Katkansky SC, Warner RW (1974) Pacific oyster disease and mortality studies in California. California Department of Fish and Game. Marine Resources Technical Report No. 25. Downloaded on March 3, 2020 from [http://aquaticcommons.org/678/1/Technical\\_Report\\_1974\\_No.\\_25\\_A.pdf](http://aquaticcommons.org/678/1/Technical_Report_1974_No._25_A.pdf).
- Keppler CJ, Hoguet J, Smith K, Ringwood AH, Lewitus AJ (2005) Sublethal effects of the toxic alga *Heterosigma akashiwo* on the southeastern oyster (*Crassostrea virginica*). *Harmful Algae* 4:275–285. <https://doi.org/10.1016/j.hal.2004.05.002>
- Kimes NE, Grim CJ, Johnson WR, Hasan NA, Tall BD, Kothary MH, Kiss H, Munk AC, Tapia R, Green L, Detter C, Bruce DC, Brettin TS, Colwell RR, Morris PJ (2012) Temperature regulation of virulence factors in the pathogen *Vibrio coralliiticyus*. *ISME J* 6:835–846. <https://doi.org/10.1038/ismej.2011.154>
- King WL, Jenkins C, Seymour JR, Labbate M (2019a) Oyster disease in a changing environment: decrypting the link between pathogen, microbiome, and environment. *Mar Environ Res* 143:124–140. <https://doi.org/10.1016/j.marenvres.2018.11.007>
- King WL, Jenkins C, Go J, Siboni N, Seymour JR, Labbate M (2019b) Characterisation of the Pacific oyster microbiome during a summer mortality event. *Microbiol Ecol* 77:502–512. <https://doi.org/10.1007/s00248-018-1226-9>
- King WL, Siboni N, Kahle T, Green TJ, Labbate M, Seymour JR (2019c) A new high throughput sequencing assay for characterizing the diversity of natural *Vibrio* communities and its application to a Pacific oyster mortality event. *Front Microbiol* 10:2907. <https://doi.org/10.3389/fmicb.2019.02907>

- King WL, Siboni N, Williams NL, Kahlke T, Nguyen KV, Jenkins C, Dove M, O'Connor W, Seymour JR, Labbate M (2019) Variability in the composition of Pacific oyster microbiomes across oyster families exhibiting different levels of susceptibility to OsHV-1  $\mu$ var disease. *Front Microbiol* 10:473. <https://doi.org/10.3389/fmicb.2019.00473>
- Labreuche Y, Lambert C, Soudant P, Boulo V, Huvet A, Nicolas JL (2006a) Cellular and molecular hemocyte responses of the Pacific oyster, *Crassostrea gigas*, following bacterial infection with *Vibrio aestuarianus* strain 01/32. *Microbes Infect* 8:2715–2724. <https://doi.org/10.1016/j.micinf.2006.07.020>
- Labreuche Y, Soudant P, Goncalves M, Lambert C, Nicolas JL (2006b) Effects of extracellular products from the pathogenic *Vibrio aestuarianus* strain 01/32 on lethality and cellular immune responses of the oyster *Crassostrea gigas*. *Dev Comp Immunol* 30:367–379. <https://doi.org/10.1016/j.dci.2005.05.003>
- Labreuche Y, Le Roux F, Henry J, Zatylny C, Huvet A, Lambert C, Soudant P, Mazel D, Nicolas JL (2010) *Vibrio aestuarianus* zinc metalloprotease causes lethality in the Pacific oyster *Crassostrea gigas* and impairs the host cellular immune defenses. *Fish Shellfish Immunol* 29:753–758. <https://doi.org/10.1016/j.fsi.2010.07.007>
- Lacoste A, Jalabert F, Malham S, Cueff A, Gélébart F, Cordevant C, Lange M, Poulet SA (2001) A *Vibrio splendidus* strain is associated with summer mortality of juvenile oysters *Crassostrea gigas* in the Bay of Morlaix. *Dis Aquat Organ* 46:139–145. <https://doi.org/10.3354/dao046139>
- Lenth R, Signmann H, Love J, Buerkner P, Herve M (2020) Estimated marginal means, aka least-squares means. Package 'emmeans' for the statistical software R. Downloaded on March 3, 2020 from <https://github.com/rvlenth/emmeans>
- Li Y, Qin JG, Abbott CA, Li X, Benkendorff K (2007) Synergistic impacts of heat shock and spawning on the physiology and immune health of *Crassostrea gigas*: an explanation for summer mortality in Pacific oysters. *Phys Reg Integr Comp Physiol* 293:2353–2362. <https://doi.org/10.1152/ajpregu.00463.2007>
- Lipovsky VP, Chew KK (1972) Mortality of Pacific oysters (*Crassostrea gigas*): the influence of temperature and enriched seawater on survival. *Proc Nat Shellfish Ass* 62:72–82. <https://www.biodiversitylibrary.org/page/2164272#page/84/mode/1up>
- Lokmer A, Wegner KM (2015) Hemolymph microbiome of Pacific oysters in response to temperature, temperature stress and infection. *ISME J* 9:670–682. <https://doi.org/10.1038/ismej.2014.160>
- Malham SK, Cotter E, O'Keeffe S, Lynch S, Culloty SC, King JW, Latchford JW, Beaumont AR (2009) Summer mortality of the Pacific oyster, *Crassostrea gigas*, in the Irish Sea: the influence of temperature and nutrients on health and survival. *Aquaculture* 287:128–138. <https://doi.org/10.1016/j.aquaculture.2008.10.006>
- Palmer JM, Jusino MA, Banik MT, Lindner DL (2018) Non-biological synthetic spike-in controls and the AMPtk software pipeline improve mycobiome data. *PeerJ* 6:e4925. <https://doi.org/10.7717/peerj.4925>
- Parizadeh L, Tourbiez D, Garcia C, Haffner P, Dégremont L, Le Roux F, Tavers M (2018) Ecologically realistic model of infection for exploring the host damage caused by *Vibrio aestuarianus*. *Environ Microbiol* 20:4343–4355. <https://doi.org/10.1111/1462-2920.14350>
- Pauley G, Raay B, Trout D (1988) Species profiles: life histories and environmental requirements of coastal fishes and invertebrates (Pacific Northwest) – Pacific oyster. U.S. Fish wildlife biological report. U.S. Army Corps of Engineers. 82:11–82. Downloaded on March 3, 2020 from <https://apps.dtic.mil/dtic/tr/fulltext/u2/a203409.pdf>
- Perdue JA (1983) The relationship between the gametogenic cycle of the Pacific oyster, *C. gigas*, and the summer mortality phenomenon in strains of selectively bred oysters. Doctoral Dissertation. University of Washington.
- Perdue JA, Beattie JH, Chew KK (1981) Relationships between gametogenic cycle and summer mortality phenomenon in the Pacific oyster (*Crassostrea gigas*) in Washington state. *J Shellfish Res* 1:9–16. <https://www.biodiversitylibrary.org/page/2156379#page/15/mode/1up>
- QGIS (2020) QGIS geographical information system. Open source geospatial foundation project. Downloaded on March 4, 2020 from <https://www.qgis.org/>
- Quayle D (1988) Pacific oyster culture in British Columbia. Department of Fisheries and Oceans – Canadian Bulletin of Fisheries and Aquatic Sciences. 218. Downloaded on March 4, 2020 from <https://waves-vagues.dfo-mpo.gc.ca/Library/109165.pdf>
- R Core (2020) R Core Team. R: A language and environment for statistical computing. The R project for statistical computing, Vienna, Australia. Downloaded on March 3, 2020 from <https://www.r-project.org/>
- Royer J, Seguinéau C, Park K, Pouvreau S, Choi K, Costil K (2008) Gametogenic cycle and reproductive effort assessed by two methods in 3 age classes of Pacific oysters, *Crassostrea gigas*, reared in Normandy. *Aquaculture* 277:313–320. <https://doi.org/10.1016/j.aquaculture.2008.02.033>
- Saulnier D, De Decker S, Tourbiez D, Travers MA (2017) Development of duplex Taqman real-time PCR assay for rapid identification of *Vibrio splendidus*-related and *V. aestuarianus* strains from bacterial cultures. *J Microbiol Methods* 140:67–69. <https://doi.org/10.1016/j.mimet.2017.07.002>

- Schneider CA, Rasband WS, Eliceiri KW (2012) NIH image to ImageJ: 25 years of image analysis. *Nat Methods* 9:671–675. <https://doi.org/10.1038/nmeth.2089>
- Steele S, Mulcahy M (1999) Gametogenesis of the oyster *Crassostrea gigas* in southern Ireland. *J Mar Biol Ass UK* 79:673–686. <https://doi.org/10.1017/S0025315498000836>
- Suquet M, Malo F, Quere C, Ledu C, Le Grand J, Benabdelmouna A (2016) Gamete quality in triploid Pacific oyster (*Crassostrea gigas*). *Aquaculture* 451:11–15. <https://doi.org/10.1016/j.aquaculture.2015.08.032>
- Tison DL, Seidler RJ (1983) *Vibrio aestuarianus*: a new species isolated from estuarine waters and shellfish. *Int J Syst Bacteriol* 33:699–702. <https://doi.org/10.1099/00207713-33-4-699>
- Van Heuven S, Pierrot D, Rae JWB, Lewis E, Wallace DWR (2011) MATLAB program developed for CO<sub>2</sub> system calculations. In ORNL/CDIAC-105b, ed. Published by Carbon Dioxide Information Analysis Center Department of Energy, Oak Ridge, Tennessee, USA
- Wadsworth P, Wilson AE, Walton WC (2019) A meta-analysis of growth rate in diploid and triploid oysters. *Aquaculture* 499:9–16. <https://doi.org/10.1016/j.aquaculture.2018.09.018>
- Wendling C, Wegner K (2013) Relative contribution of reproductive investment, thermal stress and *Vibrio* infection to summer mortality phenomena in Pacific oysters. *Aquaculture* 412:88–96. <https://doi.org/10.1016/j.aquaculture.2013.07.009>
- Wendling CC, Batista FM, Wegner KM (2014) Persistence, seasonal dynamics and pathogenic potential of *Vibrio* communities from Pacific oyster hemolymph. *PLoS One* 9(4):1–12. <https://doi.org/10.1371/journal.pone.0094256>
- Wickham H (2016) *ggplot2: elegant graphics for data analysis*. Springer-Verlag New York. Downloaded on March 3, 2020 from <https://ggplot2.tidyverse.org/>

**Publisher's Note** Springer Nature remains neutral with regard to jurisdictional claims in published maps and institutional affiliations.

## Authors and Affiliations

M. W. Cowan<sup>1,2,3</sup> · C. M. Pearce<sup>2</sup> · T. J. Green<sup>3</sup> · T. Finston<sup>1</sup> · G. R. Meyer<sup>2</sup> · B. McAmmond<sup>4</sup> · J. D. Van Hamme<sup>4</sup> · E. M. Bottos<sup>4</sup> · R. Marshall<sup>5</sup> · W. Evans<sup>6</sup> · T. F. Sutherland<sup>7</sup> · P. Y. de la Bastide<sup>1</sup>

✉ C. M. Pearce  
chris.pearce@dfo-mpo.gc.ca

<sup>1</sup> Centre for Forest Biology, Department of Biology, University of Victoria, Victoria, BC V8P 5C2, Canada

<sup>2</sup> Pacific Biological Station, Fisheries and Oceans Canada, Nanaimo, BC V9T 6N7, Canada

<sup>3</sup> Centre for Shellfish Research, Vancouver Island University, Nanaimo, BC V9R 5S5, Canada

<sup>4</sup> Department of Biological Sciences, Thompson Rivers University, Kamloops, BC V2C 0C8, Canada

<sup>5</sup> Safe Food Compliance Canada Ltd., Nanaimo, BC V9T 4N6, Canada

<sup>6</sup> Hakai Institute, Heriot Bay, BC V0P 1H0, Canada

<sup>7</sup> Pacific Science Enterprise Centre, Fisheries and Oceans Canada, West Vancouver, BC V7V 1N6, Canada